Solitary Pulmonary Nodules: Detection, Characterization, and Guidance for Further Diagnostic Workup and Treatment

Yeong Joo Jeong[1,2]
Chin A. Yi[1]
Kyung Soo Lee[1]

OBJECTIVE. The purpose of our study is to improve radiologists' understanding of the clinical issues involved in making a diagnosis and to guide further diagnostic workup and treatment of solitary pulmonary nodules (SPNs).

CONCLUSION. Information on the morphologic and hemodynamic characteristics of SPNs provided by dynamic helical CT, with high specificity and reasonably high accuracy, can be used for initial assessment. PET/CT is more sensitive at detecting malignancy than dynamic helical CT, and all malignant nodules may be potentially diagnosed as malignant by both techniques. Therefore, PET/CT may be selectively performed to characterize SPNs that show indeterminate results at dynamic helical CT.

Keywords: chest imaging, dynamic CT, lung, lung neoplasms, PET/CT, screening, solitary pulmonary nodules

DOI:10.2214/AJR.05.2131

Received December 13, 2005; accepted after revision May 25, 2006.

[1]Department of Radiology and Center for Imaging Science, Samsung Medical Center, Sungkyunkwan University School of Medicine, 50, Ilwon-dong, Kangnam-gu, Seoul 135-710, South Korea. Address correspondence to K. S. Lee (kyungs.lee@samsung.com).

[2]Present address: Department of Diagnostic Radiology, Pusan National University Hospital, Pusan National University School of Medicine and Medical Research Institute, Pusan, Korea.

CME
This article is available for CME credit. See www.arrs.org for more information.

AJR 2007; 188:57–68

0361–803X/07/1881–57

CT screening has increased the detection rate of small pulmonary nodules (SPNs). The tissue characterization of subcentimeter nodules, still a challenge to radiologists, can be performed using serial volume measurements from CT. Video-assisted thoracoscopic surgery removal after nodule localization may be performed for the diagnosis and treatment of a subcentimeter nodule. In this perspective, we propose how to improve our understanding of the clinical issues involved in making a diagnosis and to guide further diagnostic workup and treatment of SPNs.

SPNs are defined as focal, round, or oval areas of increased opacity in the lung with diameters of ≤ 3 cm [1]. The characterization of SPNs is a major concern not only to radiologists but also to clinicians because malignant lesions account for only 60–80% of resected pulmonary nodules [2–4]. The goal of the radiologic evaluation of SPNs is to noninvasively differentiate benign from malignant lesions as accurately as possible. Morphologic evaluations can help differentiate benign and malignant nodules when they have typical benign or malignant features, but there is considerable overlap between benign and malignant nodules in terms of their morphologic presentations [5].

Various strategies other than morphologic evaluations have been applied to the differentiation of malignant and benign nodules, which include growth rate assessment [6], Bayesian analysis [7], and hemodynamic characteristics on dynamic helical CT [8–10]. In addition, the assessment of nodular metabolic characteristics on ^{18}F-FDG PET [11] and pathologic evaluations using transthoracic needle aspiration, transthoracic needle biopsy, or video-assisted thoracoscopic surgery have also been used for characterizing SPNs. However, no single diagnostic algorithm can be applied to all cases.

The aim of this perspective is to improve our understanding of the clinical issues involved in making a diagnosis and to guide further diagnostic workup and treatment of SPNs.

Detection

Although new diagnostic techniques have been introduced, the detection of lung nodules on imaging is difficult. CT screening has increased the detection rate of small nodular attenuations, including those of early peripheral lung cancer [12–14]. Despite the higher spatial and contrast resolutions of CT, nodular lesions are missed on chest CT. Missed lesions occur because of failures of detection. In a study by Ko et al. [15], a small nodule size of ≤ 5 mm in diameter (nodule detection sensitivity: ≤ 5 mm vs > 5 mm, 74% vs 82%), ground-glass opacity nodules (nodule detection sensitivity: ground-glass opacity vs solid, 65% vs 83%), and lesion location (nodule detection sensitivity: central vs peripheral, 61% vs 80%) were shown to be major factors that contribute to the difficulty in detecting nodules. Nodule detection can be im-

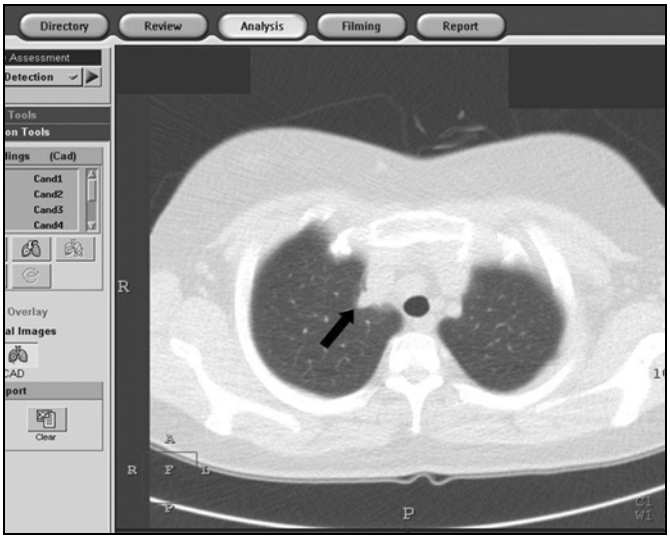

Fig. 1—Screen shot of computer-aided detection system in 44-year-old woman shows 7-mm nodule in right apex (*arrow*) adjacent to mediastinal great vessels that was not detected on computer-assisted detection system but was detected by radiologists.

proved by advances in computer-aided detection (CAD) systems that are being developed and evaluated to provide a second perspective for nodule detection on CT. The use of CAD can help improve radiologist performance for the detection of unidentified lung cancers during lung cancer screening with CT [16, 17]. However, Lee et al. [18] showed that the sensitivity of a CAD system (81%) did not significantly differ from that of radiologists (85%). Radiologists were more sensitive at detecting nodules attached to other structures (Fig. 1), whereas CAD was better at detecting isolated nodules and those that were ≤ 5 mm in diameter [18].

Morphologic Evaluation

Evaluation of the specific morphologic features of SPNs can help differentiate benign from malignant nodules. Small, smooth nodules with well-defined margins are suggestive of, but not diagnostic for, benignity; and a lobulated contour or an irregular or spiculated margin with distortion of adjacent vessels is typically associated with malignancy [5]. Diffuse, laminated, central nodular, and popcornlike calcifications within nodules suggest benignity. On the other hand, eccentric or stippled calcifications have been described in malignant nodules. Fat or calcification may be observed in up to 50% of pulmonary hamartoma [19]. In a study by Jeong et al. [10], multivariate analysis was used to identify criteria independently associated with a diagnosis of a malignant nodule that had a higher odds ratio for malignancy than other radiologic finding criteria; the criteria were a lobulated margin, a spiculated margin, and the absence of a satellite nodule. Considerable overlap exists between the internal characteristics (air bronchogram, cavitation, wall thickness, attenuation, and so forth) of benign and malignant nodules. Initial morphologic evaluations of SPNs often result in nonspecific findings and further evaluations to exclude malignancy.

When interpreting screening CT images, radiologists must search for lung nodules, differentiate malignant lesions from benign nodules, and finally, recommend follow-up actions for these detected lesions. The results of the Early Lung Cancer Action Project (ELCAP) [13] suggested that nodules with pure (nonsolid) or mixed (partially solid) ground-glass opacity on thin-section CT are more likely to be malignant than are those with solid opacity. Li et al. [20] more specifically evaluated the characteristic thin-section CT findings of malignant and benign nodules detected on screening CT. Among nodules with pure ground-glass opacity, a round shape was found more frequently for malignant lesions (65%) than for benign lesions (17%); mixed ground-glass opacity, a subtype that has ground-glass opacity in the periphery and a high-attenuation zone in the center, was seen much more often in malignant

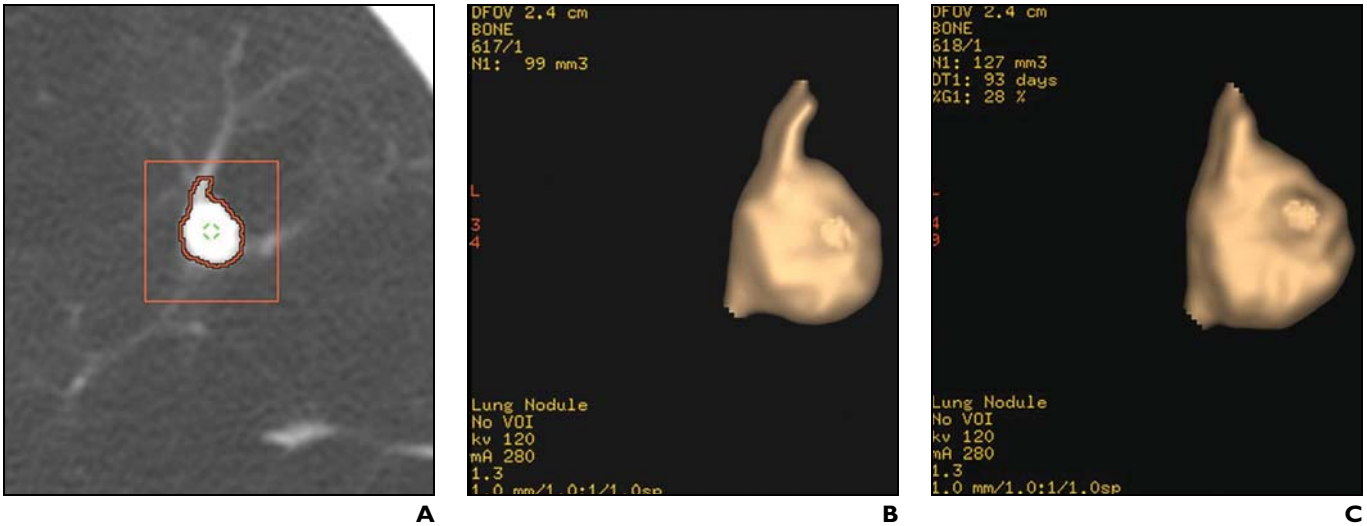

A **B** **C**

Fig. 2—Volume measurement of pulmonary nodule in 47-year-old man with lung adenocarcinoma on computer-aided detection system.
A, Application of region of interest to nodule automatically leads to volume measurement with outline delineation and nodule segmentation.
B, Volume imaging of nodule and resultant volume of 99 mm^3 are shown.
C, Volume imaging shows 127 mm^3 of nodule at follow-up after 93 days. Calculated volume doubling time is 145 days.

lesions (41%) than in benign lesions (7%). Among solid nodules, a polygonal shape or a smooth margin was present less frequently in malignant than in benign lesions.

Growth Rate Assessment

Determination of growth rate by comparing sizes on current and prior images is an important and cost-effective step in the evaluation of SPNs. The absence of detectable growth over a 2-year period of observation is a reliable criterion for establishing that a pulmonary nodule is benign [21]. Despite widespread acceptance, the value of 2-year stability for the diagnosis of a benign nodule may not be sufficient for ground-glass opacities and suspected bronchioloalveolar carcinoma [22]. In addition, it is difficult to reliably detect growth in small (< 1 cm) nodules. To overcome this limitation, it has been proposed that the growth rate of small nodules be assessed using serial volume measurements rather than diameter [23]. Computer software programs that automatically enable a nodule volume calculation have become widely available. Moreover, computer-aided 3D quantitative volume measurement methods have been developed and applied clinically [23–25] (Fig. 2).

However, all these volumetric methods are focused on solid pulmonary nodules. Few reports have dealt with nodule volumetric methods for ground-glass opacity nodules [26]. Volumetry for ground-glass opacity or semisolid (a solid nodule containing a ground-glass opacity component) nodules is more difficult than that of purely solid nodules, because these nodules have a lower nodule-to–lung parenchyma contrast ratio than solid nodules. Precise nodule volumetry methods for ground-glass opacity or semisolid nodules are under development.

Other factors that should be considered in performing in vivo nodule volumetry are motion artifacts, the presence of an adjacent normal structure, and small nodule size. Nodule volume is crucially dependent on the underlying cardiac phase. In addition, cardiovascular motion is not conveyed proportionally to various pulmonary segments. The motion is prominent in areas adjacent to the vascular structures and the heart. Nodule segmentation from adjacent normal structures is important for accurate volume measurement [26].

Bayesian Analysis

Clinical correlations continue to play a critical role in the assessment of SPNs. In an attempt to more accurately define various known risk factors, both clinical and radiologic, an increasing number of investigators have used Bayesian analysis [7]. The odds likelihood ratio form of the Bayes theorem allows the probability of malignancy to be calculated by estimating likelihood ratios for various individual radiographic and clinical characteristics derived from previous literature. Likelihood ratios are measures of the probability of a positive test result or finding in a patient with disease divided by the probability of a positive test result or finding in a patient without disease.

Using these calculations, it is possible to combine individual probabilities into an overall estimate of the odds favoring malignancy in SPNs. The hierarchy of radiologic and clinical likelihood ratios for malignancy include, in decreasing rank, a cavity of ≥ 16 mm in thickness, irregular or spiculated margin on CT scans, patient complaints of hemoptysis, a patient history of malignancy, patient age > 70 years, nodule size of 21–30 mm in diameter, nodule growth rate of 7–465 days, an ill-defined nodule on chest radiographs, patient a current smoker, and nodules with indeterminate calcification on CT scans [7]. To date, investigators have reported accuracies ranging between 53% and 96% for predicting the likelihood of malignancy [7]. Unfortunately, traditional Bayesian analysis does not include considerations of more advanced imaging techniques such as dynamic helical CT and PET, which are useful for the preoperative stratification of benign and malignant nodules.

In contrast to manual work in the Bayesian method, an artificial neural network is a computerized processing device the design of which is inspired by the design and functioning of animal brains and their components. Most neural networks have some sort of "training" rule whereby the weights of connections are adjusted on the basis of presented patterns. In differentiating malignant from benign nodules, as many as useful parameters are needed as input data for a better performance with the artificial neural network. By extracting objective features from chest radiographs and connecting them to a computerized method, Nakamura et al. [27] proved that an artificial neural network has the potential to improve the diagnostic accuracy of radiologists in the distinction of malignant and benign SPNs. If CT morphologic features are obtained and provided, a more sophisticated artificial neural network system will be provided.

Hemodynamic Characteristics on Dynamic Helical CT

The evaluation of tumor vascularity with dynamic helical CT has proved to be useful in the differentiation of malignant and benign nodules [8, 28–33]. Various threshold attenuation values have been reported to be useful for distinguishing malignant from benign nodules on dynamic helical CT [8–10, 28–33] (Table 1). The threshold attenuation values refer to the cutoff Hounsfield units of increased attenuation after contrast injection for differentiating malignant from benign nodules. Yamashita et al. [31] reported that a maximum attenuation of 20–60 H appears to be a good predictor of malignancy, and a report by Swensen et al. [8] in 2000 is also noteworthy, in that the authors reported a threshold value of 15 H produced a sensitivity of 98%, a specificity of 58%, and an accuracy of 77% for malignant nodules. Since 2000, the cutoff values for the differentiation between benign and malignant nodules have been set at 15 H.

TABLE 1: Reported Results of Dynamic CT in the Diagnosis of Solitary Pulmonary Nodules

Study	Year	No. of Cases	Cutoff Threshold	Accuracy (%)	Sensitivity (%)	Specificity (%)
Swensen et al. [28]	1992	30	20 H	97 (29/30)	100 (23/23)	86 (6/7)
Swensen et al. [29]	1995	163	19 H	93 (151/163)	100 (111/111)	77 (40/52)
Swensen et al. [30]	1996	107	20 H	85 (91/107)	98 (51/52)	73 (40/55)
Zhang and Kono [33]	1997	65	20 H	86 (56/65)	95 (40/42)	70 (16/23)
Swensen et al. [8]	2000	356	15 H	77 (274/356)	98 (167/171)	58 (107/185)
Yi et al. [9]	2004	131	30 H	78 (102/131)	99 (69/70)	54 (33/61)
Jeong et al. [10]	2005	107	WI: ≥ 25 H; WO: 5–31 H	92 (98/107)	94 (46/49)	90 (52/58)
Yi et al. [37]	2006	119	WI: ≥ 25 H; WO: 5–31 H	85 (101/119)	81 (64/79)	93 (37/40)

Note—Numbers in parentheses are actual numbers of nodules. WI = wash-in, WO = washout.

A

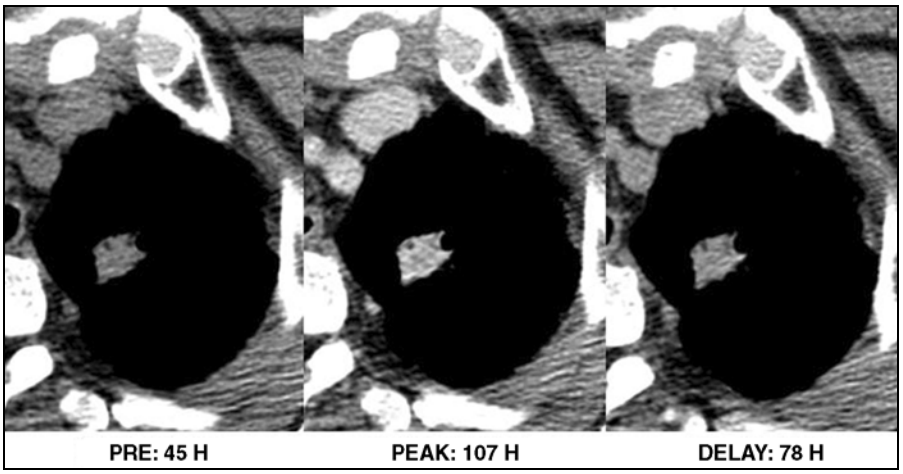

B

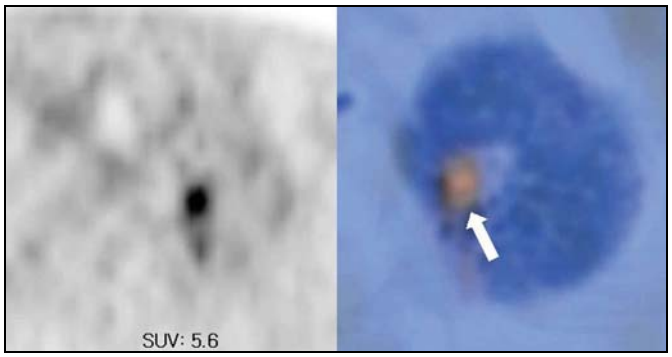

C

Fig. 3—Adenocarcinoma in 67-year-old man shows net enhancement of ≥ 25 H and washout of 5–31 H at dynamic helical CT and positive uptake at integrated PET/CT.
A, Lung window of transverse thin-section (2.5-mm collimation) CT scan shows 16-mm nodule (*arrow*) in left upper lobe has lobulated and spiculated margin.
B, Attenuation measurements on dynamic helical CT through nodule indicate malignant characteristics, showing peak enhancement of 107 H, net enhancement of 62 H, and absolute loss of enhancement (washout) of 29 H.
C, PET image (*left*) shows nodule having positive ^{18}F-FDG uptake, with maximum standardized uptake value (SUV) of 5.6. PET image was integrated with CT image (*right*). Arrow on right = nodule.

However, in these previous dynamic CT studies, in which a conventional or single-detector helical CT scanner was used, investigators acquired a single scan or a limited number of scans through the nodule at specific times (usually at 1-minute intervals, with scans obtained at 1, 2, 3, and 4 minutes after the IV injection of contrast medium) during dynamic studies [8, 30]. Therefore, a small number of CT scans obtained in a nodule at a given time may have led to partial volume effects, artifacts, and reproducibility difficulties mainly resulting from patient breath-holding variations. These limitations may also make it difficult to directly compare the attenuation values of nodules at the same level on CT scans acquired at different times. Furthermore, because images were obtained at 1-minute intervals, changes in detailed attenuation values occurring over 1-minute-long time frames would have made it difficult to determine the actual peak attenuation values and peak enhancement times.

With the advent of MDCT, we have the advantage of shorter acquisition times, greater coverage, and superior image resolution along the *z*-axis [34]. Image clusters obtained at a given time throughout a nodule can be acquired sequentially by using a helical technique at short time intervals after the IV injection of contrast medium, thus allowing the same or very similar scans to be obtained through a nodule at various times to compare extent of enhancement. In a dynamic study with MDCT [9], higher peak enhancement was obtained than in previous studies performed using conventional or single-detector helical CT [8, 28–33], and thus higher attenuation cutoff values can be used for differentiation. Actually, with a cutoff value of 30 H of net enhancement, overall diagnostic accuracy (sensitivity of 99%, specificity of 54%, positive predictive value of 71%, negative predictive value of 97%, and an accuracy of 78%) was similar to that in previous studies [8, 9, 28–31] performed using single-detector helical CT [9].

However, in early studies that focused on the early phase of dynamic CT, some overlap was found between malignant and benign nodules—for example, active granulomas and benign vascular tumors. Although the results of previous dynamic studies showed high sensitivity for the diagnosis of malignant nodules, specificities were too low. In addition, approximately 50% of indeterminate lung nodules that had an eventual benign surgical diagnosis required patient hospitalization for their surgical removal, which is expensive and involves morbidities and mortality [35, 36]. Thus, a need was created for noninvasive imaging techniques for the specific diagnosis of indeterminate lung nodules.

Evaluation of SPNs by analyzing combined wash-in and washout characteristics on dy-

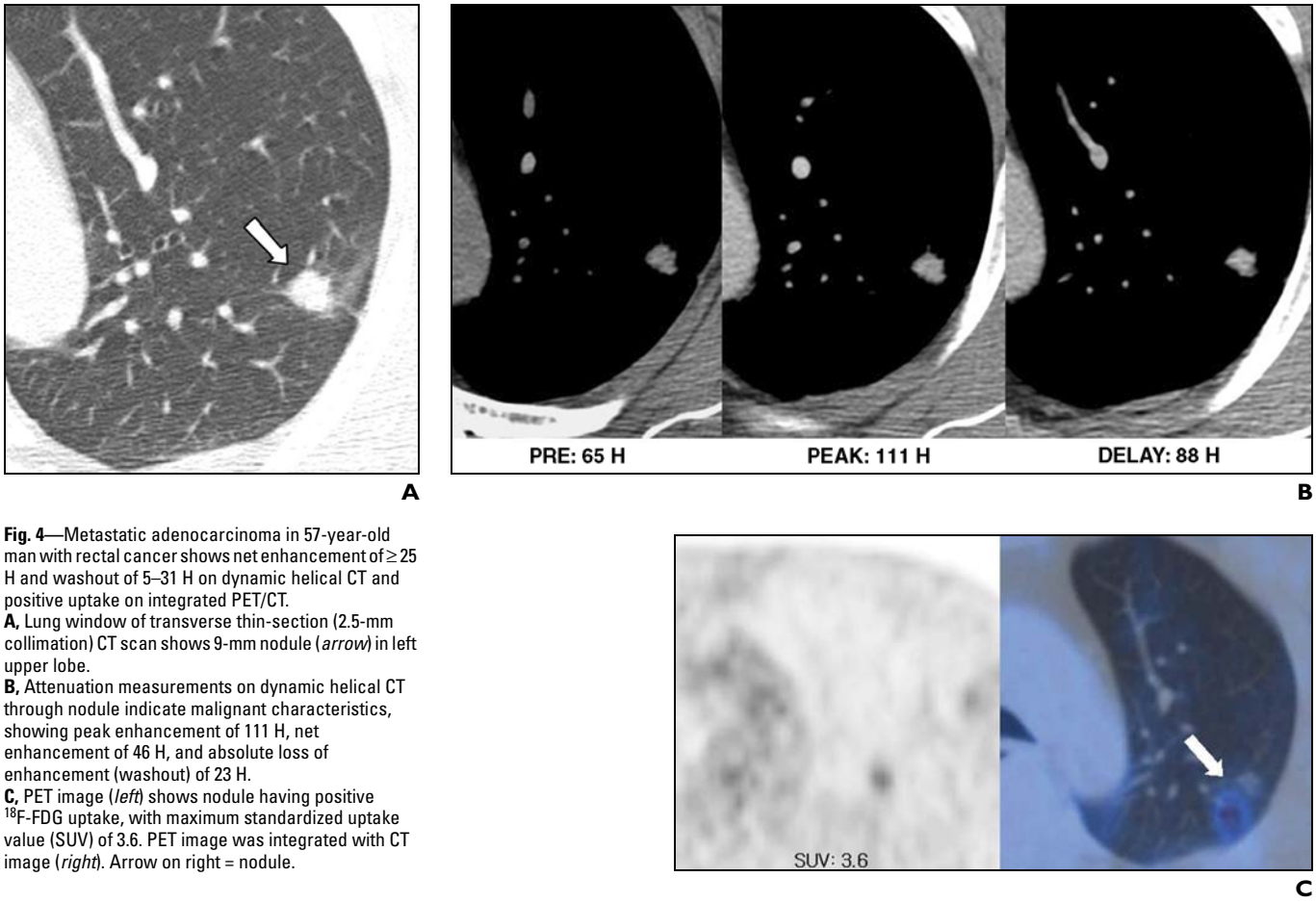

Fig. 4—Metastatic adenocarcinoma in 57-year-old man with rectal cancer shows net enhancement of ≥ 25 H and washout of 5–31 H on dynamic helical CT and positive uptake on integrated PET/CT.
A, Lung window of transverse thin-section (2.5-mm collimation) CT scan shows 9-mm nodule (*arrow*) in left upper lobe.
B, Attenuation measurements on dynamic helical CT through nodule indicate malignant characteristics, showing peak enhancement of 111 H, net enhancement of 46 H, and absolute loss of enhancement (washout) of 23 H.
C, PET image (*left*) shows nodule having positive ^{18}F-FDG uptake, with maximum standardized uptake value (SUV) of 3.6. PET image was integrated with CT image (*right*). Arrow on right = nodule.

namic helical CT allows more precise evaluations of nodule hemodynamics. In addition, the efficacy of tissue characterization has improved, and now sensitivities and specificities of more than 90% are achieved using evaluations of washout patterns in the delayed dynamic phase [10]. In a study by Jeong et al. [10], malignant nodules were characterized using a wash-in of ≥ 25 H and a washout of 5–31 H (Figs. 3 and 4). Benign nodules can be characterized using a wash-in of < 25 H, a wash-in of ≥ 25 H in combination with a washout of > 31 H, or a wash-in of ≥ 25 H and persistent enhancement without washout [10]. When diagnostic criteria of both wash-in of ≥ 25 H and washout of 5–31 H were applied for malignancy, sensitivity, specificity, and accuracy for malignancy were 81–94%, 90–93%, and 85–92%, respectively [10, 37]. According to multivariate analysis and after controlling for the effect of other diagnostic factors, Jeong et al. found that the following diagnostic criteria indicated a malignant nodule: ≥ 25 H wash-in and 5–31 H washout ($p = 0.001$; odds ratio, 25.7), lobulated margin ($p = 0.011$; odds ratio, 41.7), spiculated margin ($p = 0.006$; odds ratio, 35.3), and absence of a satellite nodule ($p = 0.004$; odds ratio, 13.8).

Metabolic Characteristics on ^{18}F-FDG PET

In an effort to improve the diagnostic accuracy of imaging pulmonary lesions, PET with ^{18}F-FDG has been used. Malignant cells have upregulated metabolisms and proliferate rapidly. Comparable enhancements of glucose and ^{18}F-FDG uptake in malignant cells have permitted malignancy to be detected on PET, which is considered an accurate, noninvasive diagnostic test, with a sensitivity of 88–96% and a specificity of 70–90% for malignant nodules [11, 38–42] (Table 2). Integrated PET/CT provides more anatomic detail and improved staging accuracy of non–small cell lung cancer versus PET alone or CT alone [43]. In a recent comparative study [37] of dynamic helical CT and integrated PET/CT for SPNs, the sensitivity, specificity, and accuracy for predicting malignant nodule on dynamic helical CT and integrated PET/CT were 81%, 93%, 85% and 96%, 88%, 93%, respectively. In that study, all malignant nodules were interpreted correctly by at least one of these two techniques, dynamic helical CT or PET/CT [37] (Figs. 3 and 4).

SPNs with increased ^{18}F-FDG uptake should be considered malignant, although false-positive results can be obtained in patients with infectious and inflammatory processes such as active tuberculosis, histoplasmosis, and rheumatoid nodules [6, 44]. The high specificity of ^{18}F-FDG PET for the diagnosis of benign lesions has important clinical usefulness. Lesions with low ^{18}F-FDG uptake may be considered benign. However, false-negative results may be seen in primary pulmonary malignancies such as carcinoids, bronchioloalveolar carcinomas, adenocarcinomas with a predominantly

TABLE 2: Reported Results of ^{18}F-FDG PET in the Diagnosis of Solitary Pulmonary Nodules

Study	Year	No. of Cases	Accuracy (%)	Sensitivity (%)	Specificity (%)
Lowe et al. [11]	1998	89	91 (81/89)	92 (55/60)	90 (26/29)
Yi et al. [37]	2006	119	93 (111/119)	96 (76/79)	88 (35/40)
Gupta et al. [38]	1996	61	92 (56/61)	93 (42/45)	88 (14/16)
Lee et al. [39]	2001	71	83 (59/71)	88 (38/43)	75 (21/28)
Dewan et al. [40]	1993	30	90 (27/30)	95 (19/20)	80 (8/10)
Herder et al. [41]	2004	36	83 (30/36)	93 (13/14)	77 (17/22)
Halley et al. [42]	2005	28	86 (24/28)	94 (17/18)	70 (7/10)

Note—Numbers in parentheses are actual numbers of nodules.

bronchioloalveolar carcinoma component (Fig. 5), and malignant SPNs of < 10 mm in diameter [11, 45, 46] (Fig. 6). Fluorine-18 FDG PET yields false-negative results in about 5% of all stage T1 lung cancers, but in only 3% of stage T1 lung cancers greater than 5 mm in diameter [47]. The long-term survival of patients with a negative PET scan for lung cancer suggests that these tumors behave indolently.

Characterization of Subcentimeter Nodules

Since the introduction of helical and MDCT, the detection of small pulmonary nodules of < 10 mm has become routine. However, characterization of nodules of < 10 mm in diameter is a challenge to radiologists. Although nodules < 10 mm in diameter have a low chance of being malignant, the reported percentage of malignancy varies according to the series [48–51]. In one report [48], nodules of < 10 mm in diameter in nonprimary lobes in lung cancer patients have only a 4% chance of being malignant. In another report, 18% of nodules < 10 mm in diameter in patients with extrathoracic malignancy were malignant [49]. On the other hand, Munden et al. [50] reported that 58% of all nodules < 10 mm in diameter were malignant and 41% of nodules < 10 mm in diameter in patients without previous malignancy represented malignancy.

Currently, serial volume measurements of nodules are regarded as the most reliable technique for the characterization of small nodules [23]. However, no report has dealt with a large number of patients. Dynamic helical CT is another reliable technique for nodule characterization. However, thin-section (≤ 1.0-mm section thickness) images with large coverage along the *z*-axis are required, especially for nodule characterization located in the lower lung zone, where the respiratory excursion of the lungs is great. PET or PET/CT is suboptimal for the characterization of subcentimeter nodules because the

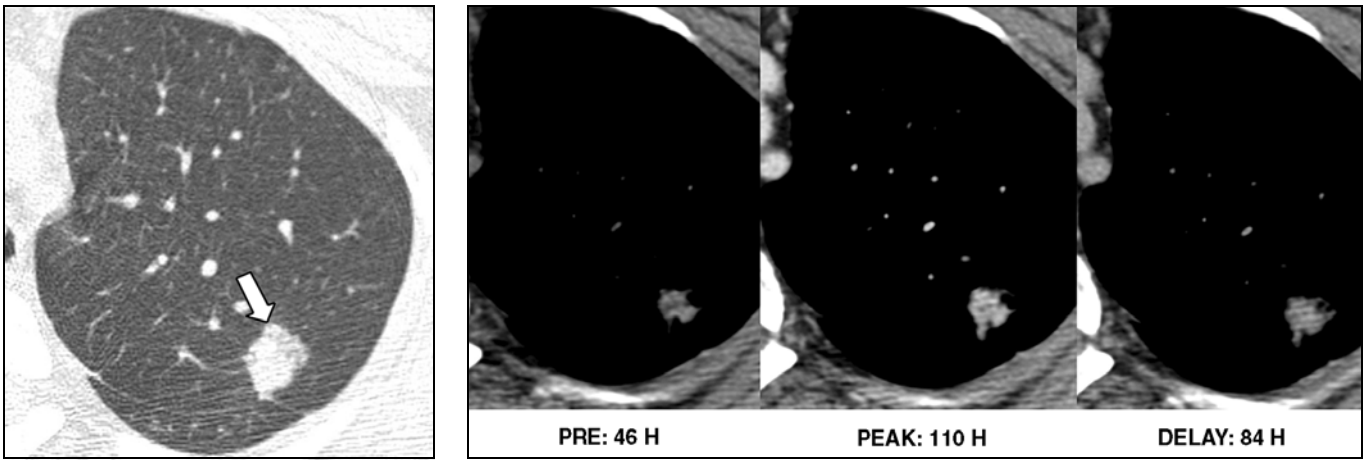

Fig. 5—Adenocarcinoma with predominantly nonmucinous bronchioloalveolar carcinoma component in 49-year-old woman shows net enhancement of ≥ 25 H and washout of 5–31 H on dynamic helical CT but little ^{18}F-FDG uptake on integrated PET/CT.
A, Lung window of transverse thin-section (2.5-mm collimation) CT scan shows 25-mm semisolid nodule (*arrow*) of mixed solid and ground-glass attenuation in left upper lobe.
B, Attenuation measurements on dynamic helical CT through nodule indicate malignant characteristics, showing peak enhancement of 110 H, net enhancement of 64 H, and absolute loss of enhancement (washout) of 26 H.
C, PET image (*left*) shows relatively little ^{18}F-FDG uptake in nodule, with maximum standardized uptake value of 1.4. PET image was integrated with CT image (*right*). Arrow on right = nodule.

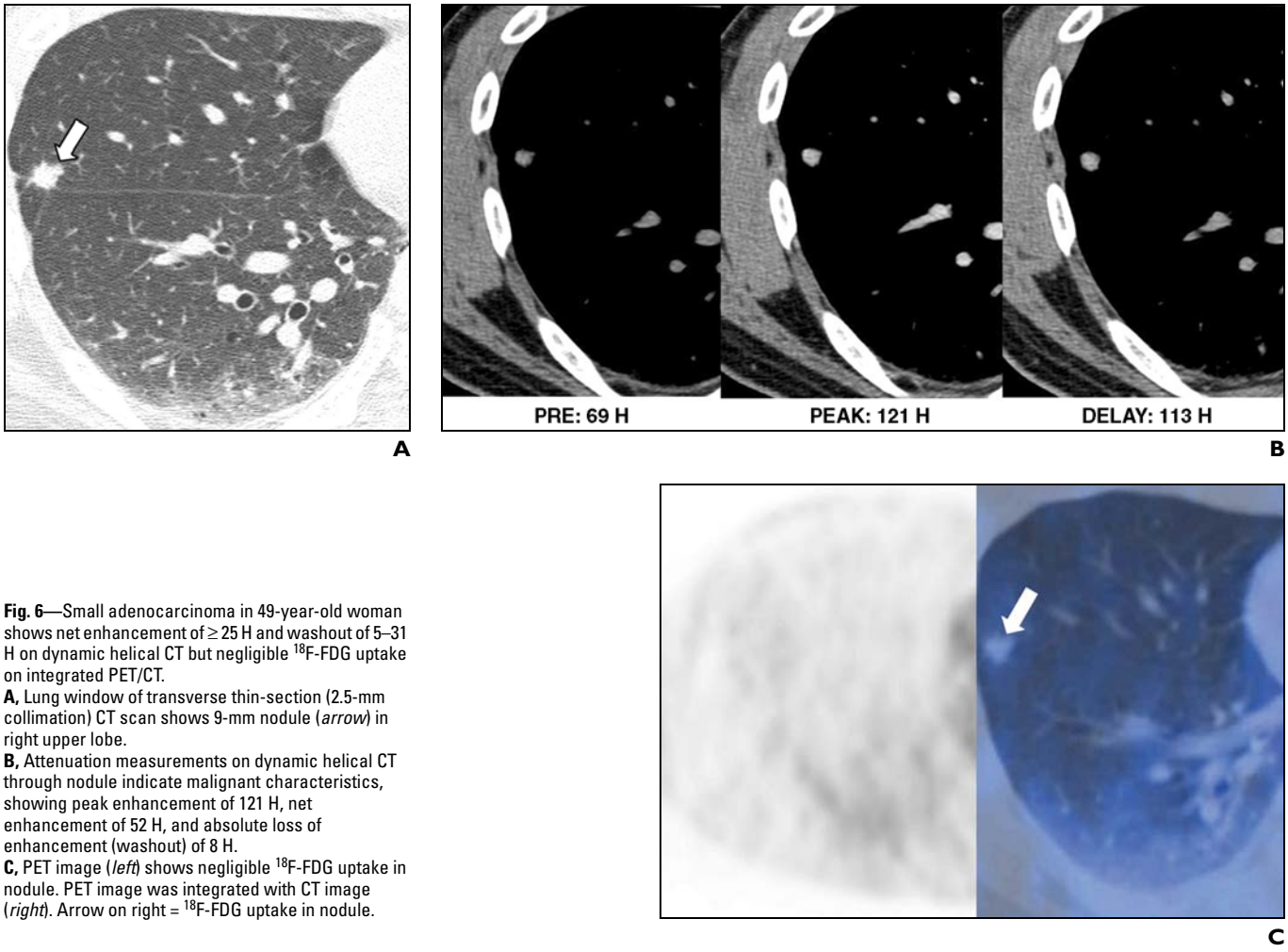

Fig. 6—Small adenocarcinoma in 49-year-old woman shows net enhancement of ≥ 25 H and washout of 5–31 H on dynamic helical CT but negligible ^{18}F-FDG uptake on integrated PET/CT.
A, Lung window of transverse thin-section (2.5-mm collimation) CT scan shows 9-mm nodule (*arrow*) in right upper lobe.
B, Attenuation measurements on dynamic helical CT through nodule indicate malignant characteristics, showing peak enhancement of 121 H, net enhancement of 52 H, and absolute loss of enhancement (washout) of 8 H.
C, PET image (*left*) shows negligible ^{18}F-FDG uptake in nodule. PET image was integrated with CT image (*right*). Arrow on right = ^{18}F-FDG uptake in nodule.

spatial resolution (currently 7 mm at most) of those techniques is insufficient for detecting malignant subcentimeter nodules [37] (Fig. 6). Therefore, it is necessary to provide practical guidelines for the follow-up and management of indeterminate small pulmonary nodules [52].

Very small (3–5 mm) well-defined nodules (sometimes called "ditzels") have been encountered more often with the advent of MDCT. Treatment decisions regarding these nodules vary depending on the patient's age, the risk of malignancy, and the risk of developing granulomatous disease. Regarding radiologists' interpretation of and management decision for these nodules [53], most radiologists recommend short-term follow-up, with less aggressive recommendations in patients who have a lower likelihood of malignancy and more aggressive recommendations in patients with a higher likelihood of malignancy.

Transthoracic Needle Biopsy or Aspiration

The use of transthoracic needle aspiration or transthoracic needle biopsy for assessing solitary nodules is well established [54–57]. The most common indication for transthoracic needle aspiration or transthoracic needle biopsy is an indeterminate SPN requiring a preoperative diagnosis, especially in patients who are unfit for surgery and who need histologic diagnosis for nonsurgical treatment planning [58]. Recent advances in transthoracic needle aspiration or biopsy, including the use of CT guidance, immediate cytopathology, the introduction of core biopsy techniques, and postbiopsy positional restrictions (to limit the incidence of pneumothoraces) have made this option still more attractive. However, the accuracy of transthoracic needle aspiration for the definitive diagnosis of benign disease has proven to be limited, typically less than 50% [56]. The effect of small lesion size (< 15 mm) is somewhat more controversial [54, 55]. Li et al. [55] reported a significant difference in the diagnostic accuracies of transthoracic needle biopsy for small and large lesions (74% vs 96%, respectively). However, more recently, Wescott et al. [54], in a study of 74 biopsies of 64 small (< 15 mm) lesions, reported a sensitivity of 93%, a specificity of 100%, and an accuracy of 95%. These discrepancies in the diagnostic accuracy of transthoracic needle biopsy for small lesions likely reflect a combination of level of experience and the number of attempted biopsies.

Although transthoracic needle aspiration or transthoracic needle biopsy is sensitive for the diagnosis of intrathoracic malignancy, the ability to differentiate between the various cell types of bronchogenic carcinoma is less well established [58]. In addi-

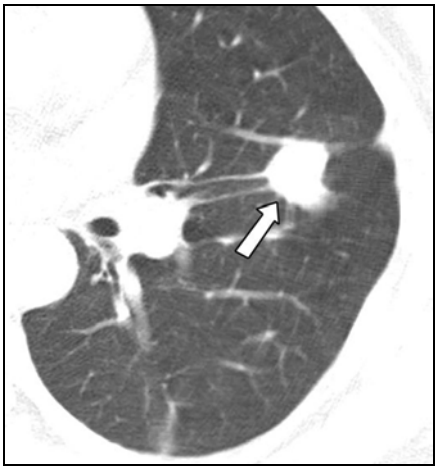

A

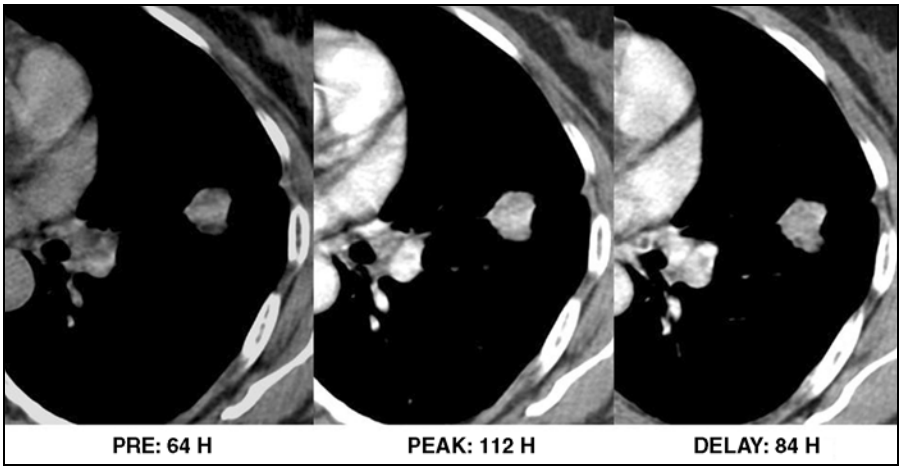

B

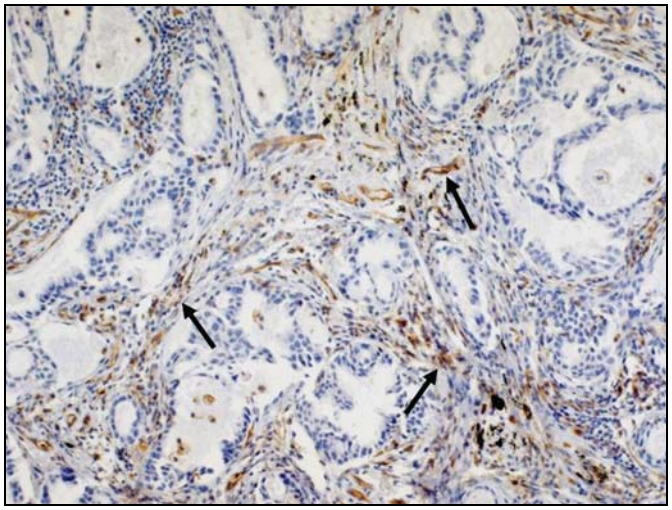

C

Fig. 7—55-year-old woman with lung adenocarcinoma. Positive correlation between extent of enhancement and microvascular density in immunostaining.
A, Lung window of transverse thin-section (2.5-mm collimation) CT scan shows 23-mm nodule in left upper lobe (*arrow*).
B, Attenuation measurements on dynamic helical CT through nodule show high enhancement: peak enhancement of 112 H, net enhancement of 48 H, and absolute loss of enhancement (washout) of 28 H.
C, Microvessel density with immunostaining for CD31 shows dark brownish stain in vessel wall (*arrows*), indicating high vessel density. (×100)

tion, transthoracic needle aspiration or biopsy may be technically limited in SPNs that are in a high apical location or too close to the hemidiaphragm.

Video-Assisted Thoracoscopic Surgery for the Diagnosis and Treatment of Small Nodules

In patients with indeterminate SPNs, video-assisted thoracoscopic surgery is indicated for lesions that are inaccessible to transthoracic needle biopsy, or when transthoracic needle biopsy is unlikely to provide a definitive benign or malignant diagnosis because of either lesion characteristics or biopsy limitations [59]. Video-assisted thoracoscopic surgery is performed, usually with the patient under general anesthesia, using a double-lumen endobronchial tube to allow ventilation of the contralateral lung. After collapse of the ipsilateral lung, three incisions are typically made and a telescope coupled to a video camera is introduced. Video-assisted thoracoscopic surgery nodule removal after nodule localization using a pulmonary nodule marking system (hookwire or tattooing with dye) is useful for the diagnosis and treatment of small SPNs. The dedicated nodule marking system is efficient in terms of localization and stable fixation of small (4–15 mm in diameter) subpleural (usually within 2 cm from the pleura or the fissure) pulmonary nodules. A small amount of pneumothorax occurs as a complication in up to 20% of patients during the placement of the nodule marking system. Once located, most nodules are removed for diagnosis or treatment. In about 5% of patients, wire dislocation may hamper nodule removal [60–63].

Prognosis of Malignant SPNs

The prevalence of nodal metastasis in patients with peripheral lung cancer—that is, stage T1 lung cancer—manifested as an SPN is considered to be low. However, several studies have reported a relatively high prevalence of mediastinal lymph node metastases [64, 65]. Aoki et al. [22] reported that adenocarcinoma appearing as localized ground-glass opacity shows slow growth, and Kim et al. [66] reported that the extent of ground-glass opacity is significantly greater in patients without recurrence, nodal metastases, or distant metastases. In addition, Jung et al. [67] suggested that the prevalence of extrathoracic metastasis is significantly less in small peripheral lung cancer with ground-glass opacity than in similar lesions without ground-glass opacity. Aoki et al. [68] evaluated the prognostic importance

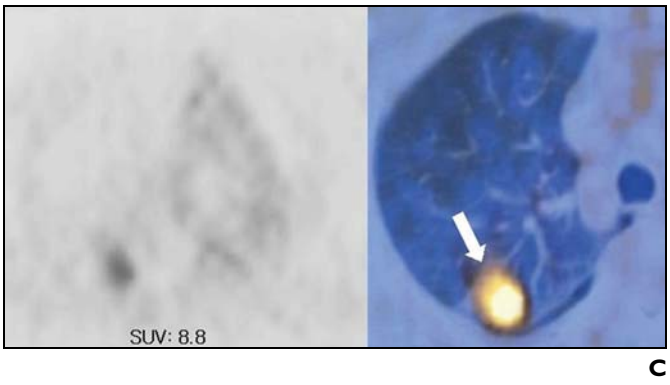

Fig. 8—Adenocarcinoma in right upper lobe in 63-year-old woman with metastases in right lower paratracheal and right hilar nodes, which were detected on dynamic helical CT but not on integrated PET/CT.
A, On transverse (5.0-mm section thickness) enhanced CT scan, lymph nodes having a short-axis diameter of < 10 mm are noticed in right lower paratracheal (*arrow*) area, representing benignity according to CT size criteria for malignant nodes.
B, Attenuation measurements on dynamic helical CT through nodule indicate probable mediastinal nodal metastasis, with peak enhancement of 123 H and net enhancement of 71 H.
C, PET (*left*) and integrated PET/CT (*right*) images show maximum standardized uptake value (SUV) of 8.8 in primary nodule (*arrow*) in right upper lobe. PET image obtained on similar level to **A** (not shown) did not show any identifiable ^{18}F-FDG uptake in mediastinal nodes.

of preoperative thin-section CT findings in peripheral lung adenocarcinoma. All adenocarcinomas smaller than 2 cm in which ground-glass opacity accounted for more than 50% of tumor volume were free of lymph node metastasis and vessel invasion, and all these patients remain alive and without recurrence 10 years later. Coarse spiculation and thickening of bronchovascular bundles around tumors were observed more frequently in tumors with lymph node metastasis or vessel invasion than in those without these findings.

The relationship between tumor size and survival in patients with stage IA non–small cell carcinoma remains a subject of debate. Patz et al. [69] and Heyneman et al. [70] found no significant correlation between the size of primary lung cancer and survival or disease stage. However, Port et al. [71] and Martini et al. [72] found that tumor size affected the survival rate of patients with stage IA tumors.

A growing malignant nodule needs its own blood supply from adjacent tissues; the blood supply is essentially required for tumor growth and metastatic spread. The blood supply process may be caused by the increased release of angiogenic factors, such as vascular endothelial growth factor, from a malignant nodule and the subsequent increase in the extent of microvessel density [9, 73]. An increased microvessel density leads to increased capillary perfusion and permeability and is frequently associated with strong enhancement of a malignant nodule on CT [9, 74]. Therefore, the extent of enhancement can be interpreted as a reflection of tumor vascularity (Fig. 7). Histologic evaluations of tumor microvessel densities and of expressions of vascular endothelial growth factor are important prognostic factors in non–small cell lung cancers [75, 76]. In other words, the likelihood of metastatic disease increases as the number of intratumoral microvessels increases in lung cancers.

Recently, Guo et al. [77] investigated the correlation between microvessel density—which is determined using various endothelial antibodies (immunostaining methods for the presence of CD31, CD105, CD34, or α-smooth muscle actin)—and ^{18}F-FDG uptake; they compared the prognostic impact of those factors in lung adenocarcinomas. They concluded that CD105 microvessel density reflects active angiogenesis, and that it is a better indicator of prognosis in patients with lung adenocarcinoma than other antibodies are (microvessel density extent determined using CD105 was negatively correlated with patient prognosis). Moreover, ^{18}F-FDG uptake at PET was found to be significantly correlated with active angiogenesis as determined by CD105 microvessel density.

Prediction of Hilar or Mediastinal Nodal Metastasis in Malignant SPNs

Efforts have been made to identify CT findings that indicate a propensity to metastasize based on analyses of morphologic characteristics, such as size or the marginal characteristics of primary tumors [69, 70, 78, 79]. However, results have been unsatisfactory and controversial,

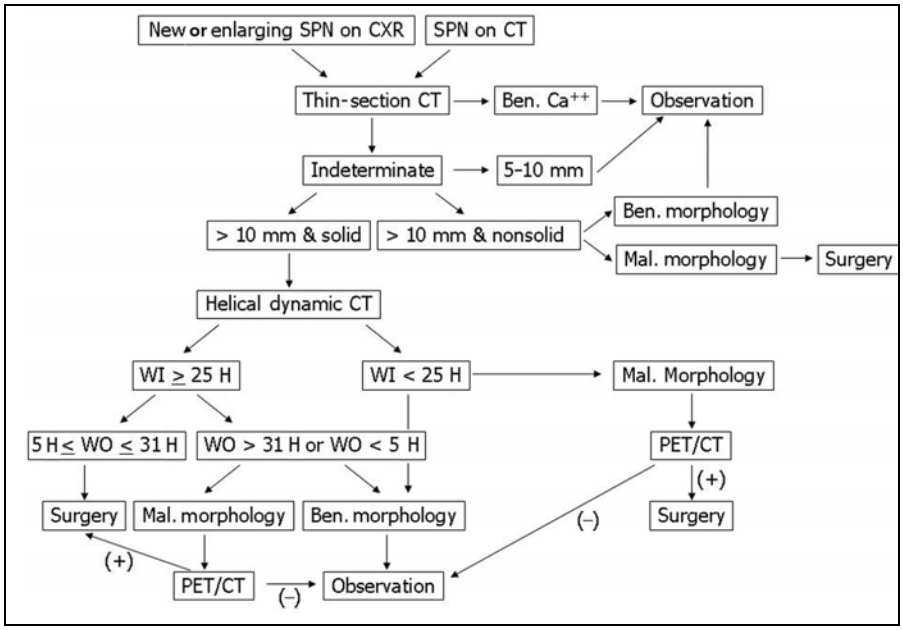

Fig. 9—Suggested algorithmic approach for solitary pulmonary nodules. SPN = solitary pulmonary nodule, CXR = chest radiography, Ben. = benign, Ca++ = calcification, WI = wash-in, Mal. = malignant, WO = washout.

especially in solid malignant nodules. Shim et al. [80] suggested that the extent of nodule enhancement is related to a propensity toward mediastinal or hilar nodal metastasis; tumor size, marginal characteristics, and the presence of necrosis or bronchovascular thickening showed no correlation with mediastinal or hilar nodal metastasis. Those authors reported that stage T1 lung cancers that show high peak enhancement or net enhancement on dynamic CT have a high likelihood of mediastinal nodal metastasis, with a sensitivity of 62%, specificity of 76%, and accuracy of 74%, after applying cutoff values of ≥ 110 H of peak enhancement, and a sensitivity of 77%, specificity of 70%, and accuracy of 71% when applying a cutoff value of 60 H of net enhancement.

According to a study by Kim et al. [81], the sensitivity, specificity, and accuracy of integrated PET/CT for mediastinal nodal staging (on a per patient basis) are 47%, 100%, and 88%, respectively, in malignant SPNs. PET/CT is still limited in terms of the detection of microscopic metastatic nodes when nodes are small in diameter [43, 82]. False-negative cases support this limitation of integrated PET/CT for the prediction of small mediastinal nodal metastasis. In the study of Kim et al. [81], in 12 of 15 false-negative cases in which no significant ^{18}F-FDG uptake occurred on PET, lymph nodes were visible in the mediastinum, but they were small, having an average short-axis diameter of 5.5 mm.

The evaluation of extent of nodule enhancement on dynamic helical CT of malignant SPNs allows better (although not statistically significant) sensitivity for the prediction of mediastinal nodal metastasis on a patient basis than PET/CT, whereas PET/CT was found to have perfect specificity and positive predictive values [80]. Therefore, mediastinoscopy may be recommended in patients with nodules that show high enhancement on dynamic helical CT even though PET/CT does not suggest the presence of mediastinal nodal metastasis (Fig. 8).

Current and Future Strategies

It is apparent that despite the considerable technical advances of imaging techniques, the diagnostic workup and management of patients with SPNs still relies on clinical perspectives, and that no single clinically based diagnostic algorithm can be applied to all cases. According to a study by Jeong et al. [10], each of the diagnostic criteria for malignancy—that is, ≥ 25 H wash-in and 5–31 H washout ($p = 0.001$; odds ratio, 25.7), a lobulated margin ($p = 0.011$; odds ratio, 41.7), a spiculated margin ($p = 0.006$; odds ratio, 35.3), and the absence of a satellite nodule ($p = 0.004$; odds ratio, 13.8)—is useful for malignant nodule diagnosis by multivariate analysis after controlling for the effects of other diagnostic factors. In light of previous results [10, 37], SPNs may be initially evaluated using dynamic helical CT, which is readily available in most institutions and which provides morphologic and hemodynamic information about nodules. PET/CT can then be used as the next step to evaluate patients with a possible malignancy.

In terms of devising diagnostic strategies for SPNs, the following questions should be raised: Should both examinations be performed despite the possible radiation hazards and the higher cost? If so, which one is technically superior, and which is the more cost-effective? On dynamic helical CT, nodules with ≥ 25 H wash-in and 5–31 H washout can be diagnosed as malignant with high specificity [10, 37]. Moreover, nodules with ≥ 25 H wash-in that have persistent enhancement without washout or with > 31 H washout can be considered benign with a 71–95% negative predictive value, although they still have the potential of being malignant. PET/CT of these patients increases diagnostic sensitivity [37]. Nodules with < 25 H wash-in have only a low possibility of being malignant (range, 0–5%) [10, 37].

However, in cases of nodules with < 25 H wash-in and nodules with ≥ 25 H wash-in and persistent enhancement without washout or with > 31 H washout, when they show malignant morphologic features of a lobulated and spiculated margin but no satellite nodules, evaluation will be improved by subsequent PET/CT. If nodules have malignant morphologic features of a lobulated or spiculated margin and no satellite lesions, PET/CT may be recommended even though a hemodynamic study suggests benignancy, especially for nodules having ≥ 25 H wash-in.

The accuracies of transthoracic needle aspiration and biopsy require elaboration. Previously described diagnostic yields of transthoracic needle aspiration or biopsy for assessing SPNs [55, 57] are lower than those obtained on PET/CT alone or on dynamic helical CT and PET/CT in combination [37], which suggests that transthoracic needle aspiration or biopsy cannot totally replace PET/CT or dynamic helical CT for the characterization of SPNs.

MDCT data may be beneficial for assessing 3D nodule perfusion and may be more accurate than the 2D analysis currently used [83]. In the future, 3D nodule enhancement and dynamic imaging may further improve the assessment of SPNs.

Conclusion

CT screening, with or without the help of a CAD system, has increased the detection rate of small nodular lesions, including that of early peripheral lung cancer. Dynamic helical

CT, providing information about morphologic and hemodynamic characteristics with high specificity and reasonably high accuracy, can be used for the initial assessment of SPNs. PET/CT is more sensitive for detecting malignancy than dynamic helical CT, and all malignant nodules may be potentially diagnosed as malignant by these two techniques. PET/CT may be selectively performed to characterize SPNs when dynamic helical CT shows inconsistent results between morphologic and hemodynamic characteristics (Fig. 9). Serial volume measurements, and thus calculation of volume doubling time, are currently the most reliable methods for the tissue characterization of subcentimeter nodules. When an SPN is highly likely to be malignant, removal of the nodule by video-assisted thorascopic surgery, after nodule localization using the pulmonary nodule marking system, may be performed for diagnosis and treatment.

References

1. Khouri NF, Meziane MA, Zerhouni EA, Fishman EK, Siegelman SS. The solitary pulmonary nodule: assessment, diagnosis, and management. *Chest* 1987; 91:128–133
2. Zerhouni EA, Stitik FP, Siegelman SS, et al. CT of the pulmonary nodule: a cooperative study. *Radiology* 1986; 160:319–327
3. Ward HB, Pliego M, Diefenthal HC, Humphrey EW. The impact of phantom CT scanning on surgery for the solitary pulmonary nodules. *Surgery* 1989; 106:734–738
4. Midthun DE, Swensen SJ, Jett JR. Approach to the solitary pulmonary nodule. *Mayo Clin Proc* 1993; 68:378–385
5. Erasmus JJ, Connolly JE, McAdams HP, Roggli VL. Solitary pulmonary nodules. Part I. Morphologic evaluation for differentiation of benign and malignant lesions. *RadioGraphics* 2000; 20:43–58
6. Erasmus JJ, McAdams HP, Connolly JE. Solitary pulmonary nodules. Part II. Evaluation of the indeterminate nodule. *RadioGraphics* 2000; 20:59–66
7. Gurney JW. Determining the likelihood of malignancy in solitary pulmonary nodules with Bayesian analysis. Part I. Theory. *Radiology* 1993; 186:405–413
8. Swensen SJ, Viggiano RW, Midthun DE, et al. Lung nodule enhancement at CT: multicenter study. *Radiology* 2000; 214:73–80
9. Yi CA, Lee KS, Kim EA, et al. Solitary pulmonary nodules: dynamic enhanced multi-detector row CT study and comparison with vascular endothelial growth factor and microvessel density. *Radiology* 2004; 233:191–199
10. Jeong YJ, Lee KS, Jeong SY, et al. Solitary pulmonary nodule: characterization with combined wash-in and washout features at dynamic multi-detector row CT. *Radiology* 2005; 237:675–683
11. Lowe VJ, Fletcher JW, Gobar L, et al. Prospective investigation of positron emission tomography in lung nodules. *J Clin Oncol* 1998; 16:1075–1084
12. Henschke CI, Naidich DP, Yankelevitz DF, et al. Early Lung Cancer Action Project: initial findings on repeat screenings. *Cancer* 2001; 92:153–159
13. Henschke CI, Yankelevitz DF, Mirtcheva R, et al. CT screening for lung cancer: frequency and significance of part-solid and nonsolid nodules. *AJR* 2002; 178:1053–1057
14. Lee IJ, Gamsu G, Czum J, Wu N, Johnson R, Chakrapani S. Lung nodule detection on chest CT: evaluation of a computer-aided detection (CAD) system. *Korean J Radiol* 2005; 6:89–93
15. Ko JP, Rusinek H, Naidich DP, et al. Wavelet compression of low-dose chest CT data: effect on lung nodule detection. *Radiology* 2003; 228:70–75
16. Li F, Arimura H, Suzuki K, et al. Computer-aided detection of peripheral lung cancers missed at CT: ROC analyses without and with localization. *Radiology* 2005; 237:684–690
17. Armato SG, Li F, Giger ML, MacMahon H, Sone S, Doi K. Lung cancer: performance of automated lung nodule detection applied to cancers missed in a CT screening program. *Radiology* 2002; 225:685–692
18. Lee JW, Goo JM, Lee HJ, Kim JH, Kim S, Kim YT. The potential contribution of a computer-aided detection system for lung nodule detection in multidetector row computed tomography. *Invest Radiol* 2004; 39:649–655
19. Siegelman SS, Khouri NF, Scott WW, et al. Pulmonary hamartoma: CT findings. *Radiology* 1986; 160:313–317
20. Li F, Sone S, Abe H, Macmahon H, Doi K. Malignant versus benign nodules at CT screening for lung cancer: comparison of thin-section CT findings. *Radiology* 2004; 233:793–798
21. Nathan MH, Collins VP, Adams RA. Differentiation of benign and malignant pulmonary nodules by growth rate. *Radiology* 1962; 79:221–232
22. Aoki T, Nakata H, Watanabe H, et al. Evolution of peripheral lung adenocarcinomas: CT findings correlated with histology and tumor doubling time. *AJR* 2000; 174:763–768
23. Yankelevitz DF, Reeves AP, Kostis WJ, Zhao B, Henschke CI. Small pulmonary nodules: volumetrically determined growth rates based on CT evaluation. *Radiology* 2000; 217:251–256
24. Wormanns D, Kohl G, Klotz E, et al. Volumetric measurements of pulmonary nodules at multi-row detector CT: in vivo reproducibility. *Eur Radiol* 2004; 14:86–92
25. Revel MP, Lefort C, Bissery A, et al. Pulmonary nodules: preliminary experience with three-dimensional evaluation. *Radiology* 2004; 231:459–466
26. Ko JP, Rusinek H, Jacobs EL, et al. Small pulmonary nodules: volume measurement at chest CT—phantom study. *Radiology* 2003; 228:864–870
27. Nakamura K, Yoshida H, Engelmann R, et al. Computerized analysis of the likelihood of malignancy in solitary pulmonary nodules with use of artificial neural networks. *Radiology* 2000; 214:823–830
28. Swensen SJ, Morin RL, Schueler BA, et al. Solitary pulmonary nodule: CT evaluation of enhancement with iodinated contrast material—a preliminary report. *Radiology* 1992; 182:343–347
29. Swensen SJ, Brown LR, Colby TV, Weaver AL. Pulmonary nodules: CT evaluation of enhancement with iodinated contrast material. *Radiology* 1995; 194:393–398
30. Swensen SJ, Brown LR, Colby TV, Weaver AL, Midthun DE. Lung nodule enhancement at CT: prospective findings. *Radiology* 1996; 201:447–455
31. Yamashita K, Matsunobe S, Tsuda T, et al. Solitary pulmonary nodule: preliminary study of evaluation with incremental dynamic CT. *Radiology* 1995; 194:399–405
32. Yamashita K, Matsunobe S, Takahashi R, et al. Small peripheral lung carcinoma evaluated with incremental dynamic CT: radiologic–pathologic correlation. *Radiology* 1995; 196:401–408
33. Zhang M, Kono M. Solitary pulmonary nodules: evaluation of blood flow patterns with dynamic CT. *Radiology* 1997; 205:471–478
34. Hu H, He HD, Foley WD, Fox SH. Four multidetector-row helical CT: image quality and volume coverage speed. *Radiology* 2000; 215:55–62
35. Mack MJ, Hazelrigg SR, Landreneau RJ, Acuff TE. Thoracoscopy for the diagnosis of the indeterminate solitary pulmonary nodule. *Ann Thorac Surg* 1993; 56:825–830
36. Bernard A. Resection of pulmonary nodules using video-assisted thoracic surgery. The Thorax Group. *Ann Thorac Surg* 1996; 61:202–204
37. Yi CA, Lee KS, Kim B-T, et al. Tissue characterization of solitary pulmonary nodule: comparative study between helical dynamic CT and integrated PET/CT. *J Nucl Med* 2006; 47:443–450
38. Gupta NC, Maloof J, Gunel E. Probability of malignancy in solitary pulmonary nodules using fluorine-18-FDG and PET. *J Nucl Med* 1996; 37:943–948
39. Lee J, Aronchick JM, Alavi A. Accuracy of F-18 fluorodeoxyglucose positron emission tomography for the evaluation of malignancy in patients presenting with new lung abnormalities: a retrospective review. *Chest* 2001; 120:1791–1797
40. Dewan NA, Gupta NC, Redepenning LS, Phalen JJ, Frick MP. Diagnostic efficacy of PET-FDG imaging in solitary pulmonary nodules: potential role in evaluation and management. *Chest* 1993; 104:997–1002

41. Herder GJ, Golding RP, Hoekstra OS, et al. The performance of ^{18}F-fluorodeoxyglucose positron emission tomography in small solitary pulmonary nodules. *Eur J Nucl Med Mol Imaging* 2004; 31:1231–1236
42. Halley A, Hugentobler A, Icard P, et al. Efficiency of ^{18}F-FDG and ^{99m}Tc-depreotide SPECT in the diagnosis of malignancy of solitary pulmonary nodules. *Eur J Nucl Med Mol Imaging* 2005; 32:1026–1032
43. Lardinois D, Weder W, Hany TF, et al. Staging of non–small-cell lung cancer with integrated positron emission tomography and computed tomography. *N Engl J Med* 2003; 348:2500–2507
44. Goo JM, Im JG, Do KH, et al. Pulmonary tuberculoma evaluated by means of FDG PET: findings in 10 cases. *Radiology* 2000; 216:117–121
45. Erasmus JJ, McAdams HP, Patz EF Jr, Coleman RE, Ahuja V, Goodman PC. Evaluation of primary pulmonary carcinoid tumors using FDG PET. *AJR* 1998; 170:1369–1373
46. Higashi K, Ueda Y, Seki H, et al. Fluorine-18-FDG PET imaging is negative in bronchioloalveolar lung carcinoma. *J Nucl Med* 1998; 39:1016–1020
47. Lee KS, Jeong YJ, Han J, Kim BT, Kim H, Kwon OJ. T1 non–small cell lung cancer: imaging and histopathologic findings and their prognostic implications. *RadioGraphics* 2004; 24:1617–1636
48. Kim YH, Lee KS, Primack SL, et al. Small pulmonary nodules on CT accompanying surgically resectable lung cancer: likelihood of malignancy. *J Thorac Imaging* 2002; 17:40–46
49. Chalmers N, Best JJ. The significance of pulmonary nodules detected by CT but not by chest radiography in tumor staging. *Clin Radiol* 1991; 44:410–412
50. Munden RP, Pugatch RD, Liptay MJ, Sugarbaker DJ, Le LU. Solitary pulmonary lesions detected at CT: clinical importance. *Radiology* 1997; 202:105–110
51. Yuan Y, Matsumoto T, Hiyama A, et al. The probability of malignancy in small pulmonary nodules coexisting with potentially operable lung cancer detected by CT. *Eur Radiol* 2003; 13:2447–2453
52. MacMahon H, Austin JH, Gamsu G, et al. Guidelines for management of small pulmonary nodules detected on CT scans: a statement from the Fleischner Society. *Radiology* 2005; 237:395–400
53. Munden RF, Hess KR. "Ditzels" on chest CT: survey of members of the Society of Thoracic Radiology. *AJR* 2001; 176:1363–1369
54. Westcott JL, Rao N, Colley DP. Transthoracic needle biopsy of small pulmonary nodules. *Radiology* 1997; 202:97–103
55. Li H, Boiselle PM, Shepard JO, Trotman-Dickenson B, McLoud TC. Diagnostic accuracy and safety of CT-guided percutaneous needle aspiration biopsy of the lung: comparison of small and large pulmonary nodules. *AJR* 1996; 167:105–109
56. Fraser RS. Transthoracic needle aspiration: the benign diagnosis. *Arch Pathol Lab Med* 1991; 115:751–761
57. Yankelevitz DF, Henschke CI, Koizumi JH, Altorki NK, Libby D. CT-guided transthoracic needle biopsy of small solitary pulmonary nodules. *Clin Imaging* 1997; 21:107–110
58. Klein JS, Zarka MA. Transthoracic needle biopsy: an overview. *J Thorac Imaging* 1997; 12:232–249
59. Kaiser LR, Shrager JB. Video-assisted thoracic surgery: the current state of the art. *AJR* 1995; 165:1111–1117
60. Burdine J, Joyce LD, Plunkett MB, Inampudi S, Kaye MG, Dunn DH. Feasibility and value of video-assisted thoracoscopic surgery wedge excision of small pulmonary nodules in patients with malignancy. *Chest* 2002; 122:1467–1470
61. Partik BL, Leung AN, Muller MR, et al. Using a dedicated lung-marker system for localization of pulmonary nodules before thoracoscopic surgery. *AJR* 2003; 180:805–809
62. Hanninen EL, Langrehr J, Raakow R, et al. Computed tomography-guided pulmonary nodule localization before thoracoscopic resection. *Acta Radiol* 2004; 45:284–288
63. Eichfeld U, Dietrich A, Ott R, Kloeppel R. Video-assisted thoracoscopic surgery for pulmonary nodules after computed tomography-guided marking with a spiral wire. *Ann Thorac Surg* 2005; 79:313–316
64. Glazer GM, Orringer MB, Gross BH, Quint LE. The mediastinum in non–small cell lung cancer: CT–surgical correlation. *AJR* 1984; 142:1101–1105
65. Primack SL, Lee KS, Logan PM, Miller RR, Muller NL. Bronchogenic carcinoma: utility of CT in the evaluation of patients with suspected lesions. *Radiology* 1994; 193:795–800
66. Kim EA, Johkoh T, Lee KS, et al. Quantification of ground-glass opacity on high-resolution CT of small peripheral adenocarcinoma of the lung: pathologic and prognostic implications. *AJR* 2001; 177:1417–1422
67. Jung KJ, Lee KS, Kim H, et al. T1 lung cancer at CT: frequency of extrathoracic metastases. *J Comput Assist Tomogr* 2000; 24:711–718
68. Aoki T, Tomoda Y, Watanabe H, et al. Peripheral lung adenocarcinoma: correlation of thin-section CT findings with histologic prognostic factors and survival. *Radiology* 2001; 220:803–809
69. Patz EF, Rossi S, Harpole DH, Herndon JE, Goodman PC. Correlation of tumor size and survival in patients with stage IA non–small cell lung cancer. *Chest* 2000; 117:1568–1571
70. Heyneman LE, Herndon JE, Goodman PC, Patz EF Jr. Stage distribution in patients with a small (< or = 3 cm) primary nonsmall cell lung carcinoma: implication for lung carcinoma screening. *Cancer* 2001; 92:3051–3055
71. Port JL, Kent MS, Korst RJ, Libby D, Pasmantier M, Altorki NK. Tumor size predicts survival within stage IA non–small cell lung cancer. *Chest* 2003; 124:1828–1833
72. Martini N, Bains MS, Burt ME, et al. Incidence of local recurrence and second primary tumors in resected stage I lung cancer. *J Thorac Cardiovasc Surg* 1995; 109:120–129
73. Fontanini G, Bigini D, Vignati S, et al. Microvessel count predicts metastatic disease and survival in non–small cell lung cancer. *J Pathol* 1995; 177:57–63
74. Miles KA. Tumour angiogenesis and its relation to contrast enhancement on computed tomography: a review. *Eur J Radiol* 1999; 30:198–205
75. Fontanini G, Vignati S, Boldrini L, et al. Vascular endothelial growth factor is associated with neovascularization and influences progression of non–small cell lung carcinoma. *Clin Cancer Res* 1997; 3:861–865
76. Volm M, Koomagi R, Mattern J. PD-ECGF, bFGF, and VEGF factor expression in non–small cell lung carcinomas and their association with lymph node metastasis. *Anticancer Res* 1999; 19:651–655
77. Guo JF, Higashi K, Takahashi T, Oguchi M, Tonami H, Yamamoto I. Microvessel density in lung adenocarcinomas: correlation with FDG uptake and survival. (abstr) *Radiology* 2005; 237(P):278
78. Shim SS, Lee KS, Kim BT, et al. Non–small cell lung cancer: prospective comparison of integrated FDG PET/CT and CT alone for preoperative staging. *Radiology* 2005; 236:1011–1019
79. Gail MH, Eagan RT, Feld R, et al. Prognostic factors in patients with resected stage I non–small cell lung cancer: a report from the Lung Cancer Study Group. *Cancer* 1984; 54:1802–1813
80. Shim SS, Lee KS, Chung MJ, Kim H, Kwon OJ, Kim S. Do hemodynamic studies of stage T1 lung cancer enable the prediction of hilar or mediastinal nodal metastasis? *AJR* 2006; 186:981–988
81. Kim BT, Lee KS, Shim SS, et al. Stage T1 non–small cell lung cancer: preoperative mediastinal nodal staging with integrated FDG PET/CT—a prospective study. *Radiology* 2006; 241:501–509
82. Takamochi K, Yoshida J, Murakami K, et al. Pitfalls in lymph node staging with positron emission tomography in non–small cell lung cancer patients. *Lung Cancer* 2005; 47:235–242
83. Ko JP. Lung nodule detection and characterization with multi-slice CT. *J Thorac Imaging* 2005; 20:196–209